

## Immobilisation of tobacco etch virus (TEV) protease on a high surface area protein nanofibril scaffold

**Jared K. Raynes**

CSIRO Agriculture and Food, 671 Sneydes Road, Werribee, Victoria 3030, Australia  
Biomolecular Interaction Centre and School of Biological Sciences, University of Canterbury, Private Bag 4800, Christchurch 8140, New Zealand

**Laura J. Domigan**

School of Biological Sciences, University of Auckland, Auckland, New Zealand  
Biomolecular Interaction Centre, Private Bag 4800, Christchurch 8140, New Zealand  
MacDiarmid Institute for Advanced Materials and Nanotechnology, Wellington 6140, New Zealand

**F. Grant Pearce**

School of Biological Sciences, University of Canterbury, Christchurch, New Zealand  
Biomolecular Interaction Centre, Private Bag 4800, Christchurch 8140, New Zealand

**Juliet A. Gerrard\***

School of Biological Sciences and School of Chemical Sciences, University of Auckland, Private Bag 92019, Auckland 1142, New Zealand  
Biomolecular Interaction Centre and School of Biological Sciences, University of Canterbury, Private Bag 4800, Christchurch 8140, New Zealand  
MacDiarmid Institute for Advanced Materials and Nanotechnology, Wellington 6140, New Zealand

---

*Tobacco etch virus (TEV) protease is widely used for the removal of poly-histidine affinity tags from proteins. In solution, it is a one-time use enzyme for tag cleavage that has low stability, and is therefore a good candidate for immobilisation. Amyloid fibrils can act as a versatile nanoscaffold by providing a large surface area for biomolecule immobilisation. Immobilisation of TEV protease to amyloid fibrils grown from the surface of a small glass bead, using physisorption, successfully immobilised active TEV protease. The bead retained activity over several uses and successfully cleaved a poly-histidine tag from several his-tagged proteins. This is first time that TEV protease has been immobilised to insulin amyloid fibrils, or any protein based support. Such functionalised surface assembled amyloid fibrils show promise as a novel nanosupport for the creation of functional bionanomaterials, for example, active surface coatings for the production of fine chemicals, chemical detoxification, or biosensing. Insulin amyloid fibrils provide a new nanosupport for the immobilisation of TEV protease, which could allow for the reuse of the enzyme, saving on production costs for recombinantly expressed poly-histidine tagged proteins.*

---

This article has been accepted for publication and undergone full peer review but has not been through the copyediting, typesetting, pagination and proofreading process which may lead to differences between this version and the Version of Record. Please cite this article as doi: 10.1002/btpr.2670

© 2018 American Institute of Chemical Engineers Biotechnol Prog

Received: Jan 21, 2018; Revised: Feb 25, 2018; Accepted: May 25, 2018

## Introduction

A major use of tobacco etch virus (TEV) protease in biotechnology is for the cleavage of affinity tags used for purification of recombinantly expressed proteins<sup>1</sup>. Tags are fused with proteins of interest, generally to assist with purification, but they can also act to increase yields, protect them from intracellular proteolysis and in the case of the maltose binding protein, aid in solubility<sup>2</sup>. Whilst there are huge benefits of tags, their incorporation on a protein of interest can hinder the activity of the tagged protein, therefore, it is generally advised to remove the tags. The main advantage of TEV protease compared to other proteases, such as Factor Xa, and thrombin, is that it is extremely selective for its recognition site, thus its accuracy ensures the protein is not cleaved incorrectly, inactivating the protein<sup>1</sup>.

TEV protease (EC number 3.4.22.44) recognises the linear epitope sequence E-Xaa-Xaa-Y-X<sub>aa</sub>-Q-(G/S), with cleavage occurring between the Q and the G/S amino acid residues. The optimal recognition site of TEV protease was shown to be ENLYFQG<sup>3</sup>, which is the sequence present in all of the cleavable poly-histidine tagged (his-tagged) proteins used in this research.

TEV protease is a prime candidate for immobilisation, because although protocols have been optimized<sup>4,5</sup>, is it reasonably difficult to purify recombinantly<sup>6</sup>, and immobilisation will allow for the reuse of the protease. The general in-solution cleavage conditions for TEV protease are at ~1-100 w/w ratio of the target protein<sup>7</sup>.

Once the reaction has taken place, the TEV protease generally needs to be separated from the cleaved target protein. If using the poly-histidine tagged TEV protease, nickel affinity chromatography can be used, but it requires removing dithiothreitol (DTT) and ethylenediaminetetraacetic acid (EDTA) (both are present in the TEV protease storage buffer) from the buffer, therefore the buffer would need to be

dialysed first<sup>5</sup>. Immobilisation could solve this problem, allowing for the simple separation of TEV protease from the target protein.

Waugh *et al.* (2010) stated “On-column (TEV protease) cleavage is possible but comparatively inefficient<sup>7</sup>”, and there have been a small number of efforts to immobilise TEV protease<sup>6,8-10</sup>. Puhl *et al.* (2009) covalently immobilised TEV protease to two insoluble supports, thiolsulfinate agarose and glutaraldehyde agarose, in which immobilised TEV protease only retained 0 or 30 % activity, respectively, compared to the enzyme in solution. The inactivation of the TEV protease was thought to be due to binding of the thiol group of a cysteine in the active site, and the GA interacting with lysine amino acid residues located near the substrate binding site. Miladi *et al.* (2012) immobilised TEV protease containing a Streptag II affinity sequence *via* affinity immobilisation on a streptavidin-agarose matrix, with a retained activity of ~81 %. This is a very good retention of activity, but examining their data closely the immobilised TEV protease has <10 % catalytic efficiency compared to the solution TEV protease. Wang *et al.* (2014) immobilised TEV protease onto magnetic nanoparticles *via* site specific (N- or C- terminus) 2-cyanobenzothiazole (CBT)-cysteine condensation reaction. The immobilisation enzyme showed a 50% reduction in activity, with immobilisation *via* the N-terminus resulting in much higher levels of activity than *via* the C-terminus. Yu *et al* (2017) successfully immobilised TEV protease to regenerated amorphous cellulose (RAC) *via* a fused cellulose-binding domain (CBD). Although the immobilised TEV protease showed reduced cleavage efficiency, improved stability (retention of 78% activity, compared to 40%) while operating at 4 °C for 10 days was observed.

Immobilised TEV protease could prove to be extremely useful, but it is clearly a difficult protein to immobilise. The selected immobilisation matrix for high loading of TEV protease at low cost is an important consideration for industrial application<sup>8</sup>.

Many different supports exist for enzyme immobilisation, and protein nanofibrils, such as amyloid fibrils, can act as a biomolecule nanoscaffold<sup>11-16</sup>. The intrinsic features of amyloid fibrils such as their nanometre size, chemical functionality arising from amino acid side chains and the ability to self-assemble, make amyloid fibrils an ideal candidate as a nanoscaffold. In this study, bovine insulin amyloid fibrils are used as a model amyloid fibril nanoscaffold. Immobilising TEV protease to surface assembled insulin amyloid fibrils could provide a solution to the inactivation immobilisation problems and loss of catalytic efficiency seen with the other TEV protease immobilisation methods, because it could allow for a large enzyme loading and create a beneficial environment for TEV protease to remain active.

## Materials and Methods

### *Materials*

Unless otherwise stated, chemicals were purchased from Sigma-Aldrich or Invitrogen. SDS PAGE densitometry analysis used GelAnalyzer<sup>17</sup> and amyloid fibril dimensions were measured using ImageJ V1.51j<sup>18</sup>.

### *Insulin protein nanofibril formation*

Insulin amyloid fibrils were formed using in-house methods modified from Nielsen *et al.*<sup>19</sup>. Bovine insulin was dissolved at a concentration of 5.8 mg/mL (1 mM) in amyloid fibril incubation buffer containing 25 mM HCl, 100 mM NaCl, pH 1.6. The insulin solution was then incubated at 60 °C for at least 24 hours. Formation of insulin amyloid fibrils was assessed by the thioflavin T (ThT) assay and transmission electron microscopy (TEM).

### *Insulin protein nanofibril fragment formation*

Bovine insulin protein nanofibrils were formed at 1 mg/mL as described above. The mature amyloid fibrils were then frozen overnight to create protein nanofibril fragments. TEM was used to confirm that fragments had been successfully produced. The fibril fragments were thawed, centrifuged at 14100 xg using an Eppendorf MiniSpin plus centrifuge and resuspended in 50 mM HEPES, pH 9.

#### ***Insulin seed formation***

Bovine insulin (1 mg/mL) was incubated at 60 °C for 80 min. The sample was then tested for ThT fluorescence to ensure amyloid formation had not occurred. The seeds were then dialysed for ~ 15 hours into 50 mM HEPES, pH 9.

#### ***Thioflavin T (ThT assay)***

ThT (2.5 mM in 50 mM tris-base, 100 mM NaCl, pH 7.5) was filtered and stored in the dark for up to a maximum of two days. ThT fluorescence was measured using a BMG Labtech FLUOstar Optima plate reader with excitation/emission filters of 450 and 485 nm, respectively<sup>20</sup>. Samples had a total volume of 200 µL containing 25 µM ThT. Three replicates of each sample were measured. Where glass beads were used, each bead was placed into a well of a 96 well plate and immersed with 200 µL containing 25 µM ThT.

#### ***Transmission electron microscopy (TEM)***

Insulin amyloid fibrils were negatively stained with filtered 1% uranyl acetate on Formvar-coated copper grids (200 mesh) and washed twice with nanopure H<sub>2</sub>O. Samples were viewed at 89,000x magnification on a Morgagni 268D TEM (FEI Company, Oregon, USA) operating at 80 kV, fitted with a 40 µm objective aperture.

### ***Glass bead surface activation***

Borosilicate glass beads (5 mm diameter; Sigma-Aldrich) were cleaned overnight in a piranha solution (70 % H<sub>2</sub>SO<sub>4</sub>, 30 % H<sub>2</sub>O<sub>2</sub>), followed by rinsing in dH<sub>2</sub>O. The beads were then treated with a 3 % (3-aminopropyl)triethoxysilane (APTS) solution in ethanol/water (95:5 v/v) for 1 hour, immersed in 99.9 % ethanol and cured at 110 °C for 1 hour. The beads were allowed to cool, then washed in 95 % ethanol followed by treatment with 20 mM N,N'-disuccinimidyl carbonate (DSC) in 50 mM NaHCO<sub>3</sub>, pH 8.5 for 3 hours. The beads were then rinsed with dH<sub>2</sub>O and left to dry prior to use.

### ***Glass bead template directed insulin amyloid fibril assembly***

Surface activated glass beads were immersed in a solution of 1 mg/mL insulin fragments or seeds at room temperature for 30 min. The beads were then rinsed twice in dH<sub>2</sub>O before being immersed in incubation buffer containing 1 mg/mL insulin for 5 hours at 50 °C. The beads were then rinsed twice with dH<sub>2</sub>O.

### ***TEV protease immobilisation on surface assembled insulin amyloid fibrils***

S219V TEV protease was recombinantly overexpressed and purified as described previously<sup>5</sup>. The preparations were homogeneous as judged by SDS-PAGE with Coomassie blue staining.

Glass beads with surface assembled insulin amyloid fibrils were immersed in TEV protease (1 mg/mL in TEV storage buffer (25 mM sodium phosphate, 200 mM NaCl, 10 % glycerol, 2 mM EDTA, 10 mM DTT, pH 8.0) for 2 hours before being rinsed 4 times with dH<sub>2</sub>O. The beads were stored at 4 °C until needed.

### ***Surface immobilised TEV poly-histidine tagged enzyme cleavage***

Wild type *E. coli* dihydrodipicolinate synthase (DHDPS), Y107W *E. coli* DHDPS, wild type *T. maritima* dihydrodipicolinate reductase (DHDPR), wild type *A. Thaliana* DHDPR, and wild type human peroxiredoxin 3 were the cleavable poly-histidine tagged enzymes used in the cleavage experiments. All of the enzymes were obtained from purified frozen laboratory stocks. All of the enzymes were diluted to ~1 mg/mL with TEV storage buffer prior to use.

Glass beads with surface assembled amyloid fibrils and immobilised TEV protease were covered with 150  $\mu$ L of one of the poly-histidine tagged enzymes containing a TEV protease cleavage site. The cleavage reaction was carried out overnight (~18 hours) at 4 °C to allow cleavage of the poly-histidine tags. The supernatant (20  $\mu$ L) was carefully pipetted off and assessed for cleavage with SDS-PAGE. The beads were then washed 5 times in dH<sub>2</sub>O ready for reuse, with another enzyme containing a cleavable poly-histidine tag.

## **Results and discussion**

### ***Characterisation of solution assembled protein nanofibril scaffold***

The routine self-assembly of bovine insulin protein nanofibrils was based on in-house method modified from Nielsen *et al.*<sup>19</sup> Briefly, bovine insulin (5.8 mg/mL, 100 mM NaCl, pH 1.6) was subjected to 60 °C and the formation of amyloid fibrils detected by monitoring the increase in ThT fluorescence upon binding to amyloid fibrils. The time-course monitoring of the formation of bovine insulin amyloid fibrils using ThT is shown in **Figure 1** (black symbols). As can be seen, there is a pronounced lag phase preceding an exponential growth phase, characteristic of amyloid fibril formation occurring by a nucleated growth mechanism<sup>21</sup>. The formed protein



nanofibrils were characterised by negative stained TEM (**Figure 2 (A)**), and have the characteristic unbranched, twisted, fibrillar morphology of amyloid fibrils<sup>20</sup>.

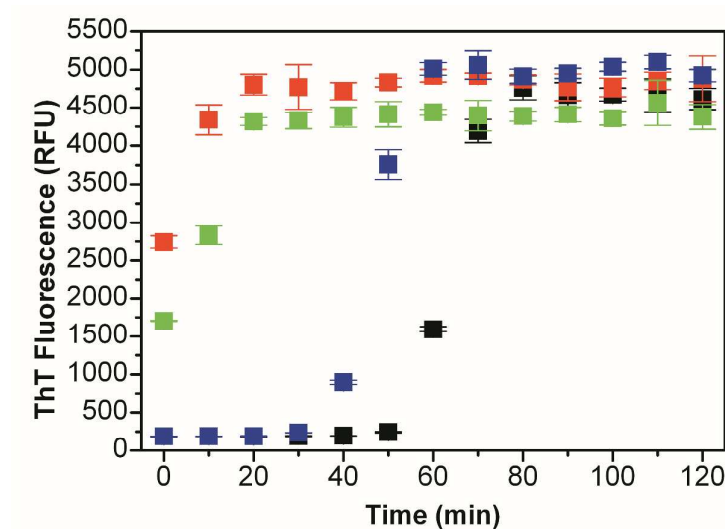


**Figure 1.** Time-course profile of insulin (1 mg/mL) amyloid fibril formation at 60 °C in the presence of 5 % insulin seeds (blue), 5 % insulin fragments (red), 5 % insulin fragments buffer exchanged (green), and insulin only (black), as monitored by ThT fluorescence. Measurements are the average of 3 replicates of each samples and the error is the standard deviation of the mean.

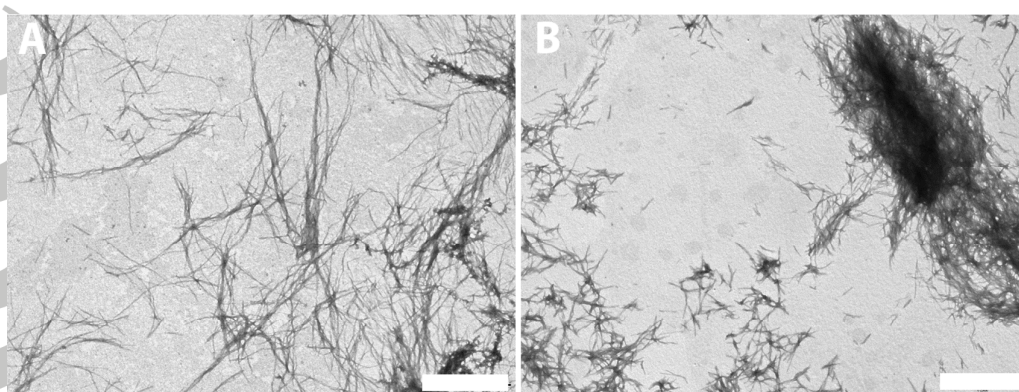


**Figure 2.** Representative TEM micrographs of insulin amyloid fibrils (A) pre-, and (B) post freezing. Scale bar 1  $\mu$ m.



### ***Surface assembled protein nanofibril scaffold***

The method to surface assemble the protein nanofibril scaffold relies on amyloid fibril formation occurring by a nucleated growth mechanism<sup>21</sup>. With this in mind, the surface assembly process is based around covalent immobilisation of protein nanofibril seeds to the surfaces, from which mature amyloid fibrils can assemble<sup>22</sup>.

The self-assembly of insulin protein nanofibrils on glass surfaces has been demonstrated *via* the covalent attachment of amyloid seeds to the glass surface<sup>23</sup>. The covalently attached seeds provide the base to which mature amyloid fibrils assemble. Surface assembled amyloid fibrils offer many potential applications for highly active surfaces by increasing the surface area of the surface to which the amyloid fibrils are assembled. Assembling the amyloid fibrils on surfaces could also provide a method of collecting the amyloid fibrils, and potentially allow for a bottom-up approach to functional bionanomaterial design.

Glass (SiO<sub>2</sub>) was chosen as a model surface because bovine insulin amyloid fibrils have previously been self-assembled from the surface of micro cover glasses<sup>23</sup>, and because the transparency of glass allows for spectrophotometric assays to be used. 5 mm glass beads were used in a 96 well sample plate to allow for high throughput sample analysis. To ensure the glass beads did not interfere with ThT fluorescence measurements, a solution of mature insulin amyloid fibrils was produced, and the fluorescence was measured with and without a glass bead in the wells of the 96 well plate (**Supplementary Figure S1**).

**Figure 3** provides an overview of the surface assembly of amyloid fibrils, towards functional bionanomaterial manufacturing – namely an enzyme immobilisation platform. First, the surface is chemically derivatised to yield an aminated surface

which amyloid seeds can be covalently attached to through their  $\epsilon$ -amino lysine or N-terminal  $\alpha$ -amino groups. As stated previously, amyloid fibril formation proceeds *via* a nucleated growth mechanism which allows the assembly of mature amyloid fibrils from the covalently bound amyloid seeds when the seeded surface is placed in a solution of native protein, and heated at low pH.

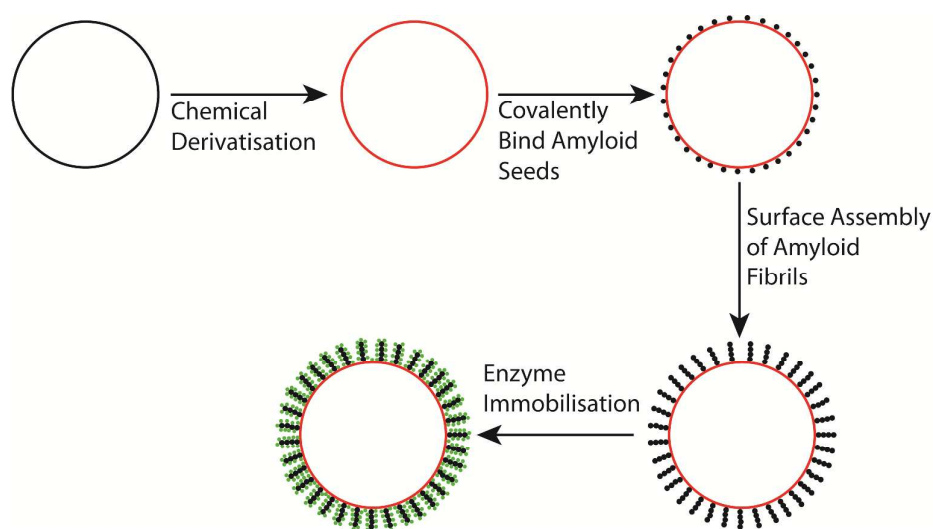


**Figure 3.** Overview of surface assembly of amyloid fibrils, and subsequent enzyme immobilisation. Firstly, glass beads are chemically derivatised with APTS and DSC to yield an activated surface that can then covalently bind amyloid seeds. Surface assembly of mature amyloid fibrils can then occur by immersion in native amyloid forming protein and heating at low pH. The surface assembled amyloid fibrils are then decorated with biomolecules by either physical adsorption or covalent coupling, depending on the biomolecule.

#### ***Derivatisation of glass surfaces***

(3-aminopropyl)triethoxysilane (APTS) is an organo-functional silane that has a non-hydrolysable amino group, and three ethoxy groups which can react with the hydroxyl

groups of glass, and can undergo a condensation reaction with itself to create an aminated surface coating<sup>24</sup>. The chemical derivation of glass with APTS, and subsequent activation with *N,N'*-disuccinimidylcarbonate (DSC), allows the covalent immobilisation of proteins through amide coupling chemistry<sup>25</sup>. This surface chemistry is readily applicable to other types of materials such as polyesters, polyamides and polycarbonates, where silanes have been used as coatings for many different applications<sup>24</sup>. The reaction between APTS and a glass surface firstly involves a hydrolysis and condensation step of APTS, followed by a hydrolysis and condensation step with the glass surface. The reaction produces an aminated surface that can then be activated with DSC *via* the formation of a succinimido carbamate to yield a surface that is able to spontaneously react with proteins, in this case insulin oligomers, through their  $\epsilon$ -amino group of lysine residues and the N-terminal  $\alpha$ -amino group<sup>25</sup>.

#### ***Template directed self-assembly of insulin amyloid fibrils***

The first step in template directed amyloid fibril growth is the covalent immobilisation of the template to the surface of the glass bead. Ha & Park (2005) used insulin seeds as their template for the surface assembly of insulin amyloid fibrils<sup>23</sup>. The seeds were created by incubating a fresh solution of insulin and heating it until the end of the lag phase, which is characteristic of a nucleated-polymerisation mechanism. The protein species formed just before the exponential growth phase are classified as seeds if they are able to eliminate the lag phase in a fresh solution of the same amyloid forming protein<sup>26</sup>. In this research insulin amyloid fragments were used as the template for the surface assembly of insulin amyloid fibrils. Fragments are mature amyloid fibrils that have been fragmented usually by mechanical means to

produce shorter amyloid fibrils<sup>27</sup>. Insulin amyloid fibril fragments were produced by a freeze-fracture method, whereby mature insulin amyloid fibrils were subjected to freezing at -20 °C overnight, then thawing<sup>28</sup>. The thawed amyloid fibril samples were then assessed for the presence of fragments using TEM before use as a template. Figure 2 shows the electron micrographs of mature insulin amyloid fibrils before freezing (A), and after freezing (B). As can be seen, the freeze-fracture method yields shorter ( $40 \text{ nm} \pm 17$ ) fragmented amyloid fibrils than the mature control sample ( $207 \text{ nm} \pm 66$ ), confirming the method can produce amyloid fragments.

Insulin amyloid fragments were chosen over insulin amyloid seeds because fragments seeded the formation of mature amyloid fibrils faster than seeds (Figure 1).

Fragmentation of the amyloid fibrils also gave more reproducible template directed amyloid fibril formation. This was because the incubation time to produce seeds before the exponential growth phase occurred varied between repetitions. When insulin amyloid fragments or fragments (buffer exchanged into 50 mM HEPES, pH 9) are added at 5 % v/v, both fragment types induce amyloid fibril formation faster, starting from time 0 when incubated at 60 °C (Figure 1). Insulin seeds added at 5 % v/v induced amyloid fibril formation at ~40 min, only slightly faster than not adding seeds. The fragments were buffer exchanged to allow the amide coupling chemistry to proceed. Buffer exchange had almost no consequence on the ability of the fragments to seed the formation of insulin amyloid fibrils (Figure 1).

The surface-activated glass beads were placed in a solution of buffer exchanged insulin amyloid fragments to covalently bind them to the glass surface *via* the amide coupling chemistry. The beads with the covalently bound insulin amyloid fragments were then placed into a solution containing dissolved insulin at pH 1.6. By heating the insulin solution at 50 °C for 5 hours, insulin amyloid fibrils will self-assemble from

the surface bound fragments. This process was monitored *via* ThT fluorescence using a 96 well plate reader (**Figure 4**). As can be seen, the glass beads which had been seeded with the fragments, then amyloid fibrils assembled, had the shortest lag phase for amyloid fibril formation. This implies that by seeding the surface of the glass beads with the fragments, template directed amyloid fibril assembly can occur. The slower amyloid formation seen with the beads can be attributed to the lower amyloid formation temperature of 50 °C, and because the native insulin has to interact with surface immobilised amyloid seeds slowing the formation process due to diffusion.

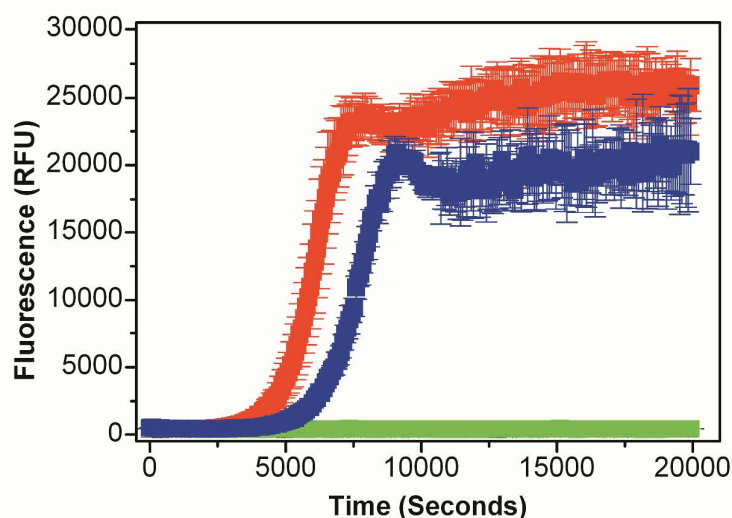


**Figure 4.** Time course profile of template directed assembly of 1 mg/mL insulin amyloid fibrils (in 25 mM HCl, 100 mM NaCl, pH 1.6 at 50 °C for 5 hours) as monitored by ThT fluorescence. Traces shown are glass beads seeded with fragments and fibrils assembled (red); not seeded and fibrils assembled (blue); seeded with fragments, no fibrils (green); not seeded and no fibrils (black – behind green). Measurements are the average of 3 replicated of each sample and the error is the standard deviation of the mean.

The beads which are not seeded with fragments still show mature amyloid fibrils are produced, but after washing the beads and measuring ThT fluorescence, only the beads which were seeded with fragments retain significant fluorescence, compared to the control without fragments or amyloid fibrils (**Figure 5**). This implies that only the seeded beads have the template directs amyloid fibrils present and that the fibrils formed in the non-seeded sample were free in solution. Appropriate controls were carried out to validate if full surface derivatisation was necessary for maximum surface assembly of the insulin amyloid fibrils (see Supplementary Information, **Figure S2**). The beads which had the full surface derivatisation, seeded with fragments, and mature amyloid fibrils assembled, had the highest ThT fluorescence and therefore the most surface assembled insulin amyloid fibrils. The sample without initial surface derivatisation (Figure S2), also shows a relatively high ThT fluorescence, suggesting there could be a relatively strong intrinsic association between the glass beads and the amyloid fragments.

Sample	ThT Fluorescence (RFU $\pm$ SD)
Not seeded, no fibrils	207 $\pm$ 17
Not seeded, fibrils	228 $\pm$ 19
Seeded, no fibrils	218 $\pm$ 18
Seeded, fibrils	1145 $\pm$ 228

**Figure 5.** ThT fluorescence (RFU) of 1 mg/mL insulin amyloid fibrils samples assembled on glass beads after washing to remove amyloid fibrils from solution phase. Measurements are the average of 3 replicates of each sample and the error is the standard deviation (SD) of the mean.

*Tobacco etch virus (TEV) protease immobilisation on surface assembled insulin amyloid fibrils*

The aim of template directed amyloid fibril growth from surfaces is to increase the available surface area for enzyme immobilisation, and to create an environment that is advantageous towards enzyme activity and stability. The use of other nanosupports such as nanoparticles, nanotubes, electrospun nanofibers and nanoporous matrices have shown the ability to increase the available surface area for enzyme immobilisation, whilst lowering mass transfer resistance<sup>14,29,30</sup>. Template directed amyloid fibril growth allows the creation of self-assembling nanomaterials, provides a means to collect amyloid fibrils, and if the surface assembled amyloid fibrils are functionalised with biomolecules, the biomolecules can be easily reused due to their surface attachment.

TEV protease was used in this research as an example of a commercially relevant biomolecule that could benefit enormously from immobilisation to an amyloid fibril nanoscaffold. TEV protease could benefit from immobilisation due to its instability outside of the cellular environment, and so that it could potentially be reused multiple times, saving on production costs.

TEV protease was immobilised onto glass beads decorated with surface assembled insulin amyloid fibrils, via physisorption to the amyloid fibrils. Following immersion of the fibril decorated beads in a 1 mg/mL solution of TEV protease, the beads were thoroughly washed to remove unbound TEV protease. To assess the amount of TEV protease immobilised, the pre-bead immersion and post-bead immersion TEV protease solutions were analysed by SDS-PAGE, with a reduction in TEV protease solution indicating immobilisation is occurring. **Figure 6 (A)** shows the SDS-PAGE gel of the pre-bead immersion TEV protease solution (lane 1), and post-bead



immersion TEV protease immobilised solutions. Densitometry analysis confirmed that the seeded + TEV protease (L2) had 15.9 % TEV adsorbed; the seeded + fibrils + TEV protease (L3) had 24.8 % TEV adsorbed; the bead + TEV protease (L4) had 38.7 % adsorbed; and the fibrils + TEV protease (L5) had 27.5 % TEV adsorbed. The TEV protease is clearly being adsorbed to all of the samples whether or not the glass beads had been seeded or not, or had amyloid fibrils assembled.

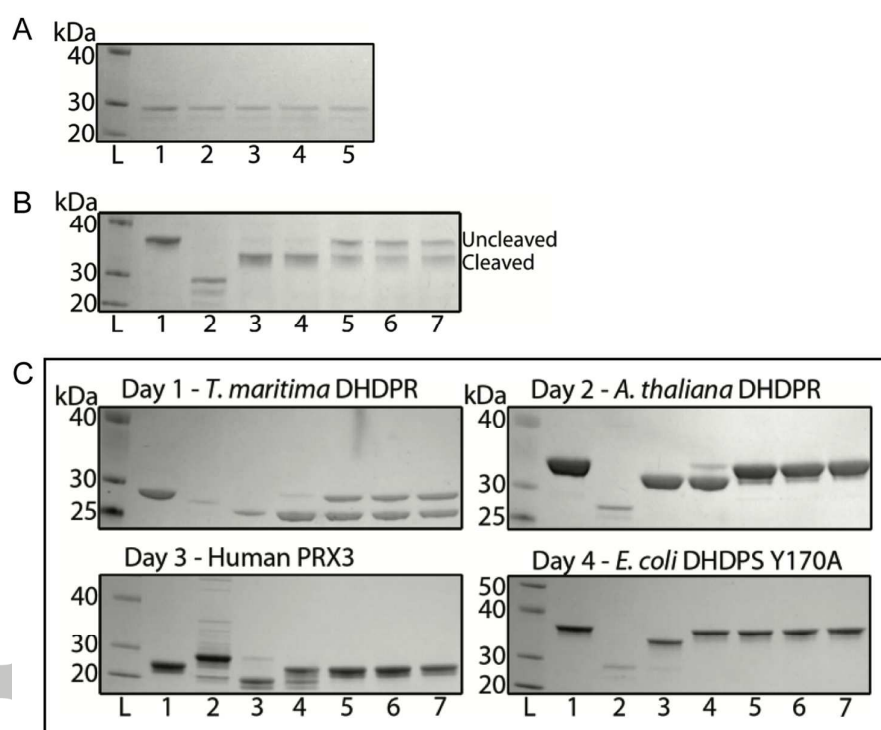


**Figure 6.** (A) SDS-PAGE gel showing the amount of TEV protease in the pre-bead immersion and post-bead immersion solutions. L – ladder; 1 – pre-bead immersion; 2 – post-bead immersion (seeded + TEV protease); 3 – post-bead immersion (seeded + fibrils + TEV protease); 4 – post-bead immersion (+ TEV protease); 5 – post-bead immersion (fibrils + TEV protease). The same amount of protein was loaded in each lane. (B) SDS-PAGE gel of *E. coli* DHDPS poly-histidine tag cleavage by

immobilised TEV protease bead samples. L – ladder; 1 – DHDPS only control; 2 – TEV only control; 3 – solution TEV protease + DHDPS cleavage control; 4 – bead (seeded + fibrils + TEV protease) DHDPS cleavage; 5 – bead (seeded + TEV protease) DHDPS cleavage; 6 – bead (fibrils + TEV protease) DHDPS cleavage; 7 – bead (+ TEV protease) DHDPS cleavage. (C) SDS-PAGE gels of poly-histidine tag cleavage by TEV protease immobilised to bead samples. For all gels the lanes contain: L – ladder; 1 – protein control; 2 – TEV protease only control; 3 – solution TEV protease protein cleavage control; 4 – bead (seeded + fibrils + TEV protease) protein cleavage; 5 – bead (seeded + TEV protease) protein cleavage; 6 – bead (fibrils + TEV protease) protein cleavage; 7 – bead (+ TEV protease) protein cleavage.

The TEV protease functionalised surface assembled amyloid fibrils were initially tested for their ability to cleave the poly-histidine tag of wild-type *E. coli* dihydrodipicolinate synthase (DHDPS). The immobilised TEV protease bead samples were put in a 1 mg/mL solution of wild-type *E. coli* DHDPS, and were incubated for 18 hours at 4 °C. The control in-solution reaction contained 10 ug of TEV protease, whilst the beads with immobilized TEV protease contained ~160-390 µg as verified from the densitometry. A fraction of each of the DHDPS solutions was carefully pipetted off without touching the glass beads, and the fractions analysed for poly-histidine tag cleavage by SDS-PAGE. As can be seen in Figure 6 (B) all of the bead samples displayed the ability to cleave the poly-histidine tag of the DHDPS, but the immobilised TEV protease bead which showed the highest activity was the bead which was seeded, amyloid fibrils assembled, and TEV protease immobilised (lane 4). All of the beads contained a higher concentration of TEV compared to the control reaction indicating that immobilization of the TEV does inhibit some of its catalytic

activity. Although, the bead sample from lane 4 was able to cleave DHDPS as well as the control in-solution reaction, indicating the immobilized TEV protease retains enough enzymatic activity to complete the reaction within 18 hours. The slight cleavage activity seen by the other bead samples could be due to the non-specific physisorption of TEV protease to the glass surface as seen in Figure 6 (A) when investigating the amount of TEV protease being immobilised to the surface assembled amyloid fibrils. However, the nanoscaffold affords a clear advantage. This is also confirmed because the TEV protease loading on the bead that was seeded and fibrils assembled did not contain the highest concentration of immobilized TEV, yet still showed the highest activity.

The TEV protease functionalised surface assembled amyloid fibrils were then tested for their ability to be reused sequentially, cleaving a different poly-histidine tagged protein on each day. It was decided to cleave a different protein each day, so that if there was any substantial contamination from a previous day's protein cleavage, a protein band corresponding to the previous days cleavage reaction would be visible on the SDS-PAGE gel. The cleavage reactions were setup as for Figure 6 (B), but after each 18 hour cleavage reaction, the beads were thoroughly washed in  $\text{dH}_2\text{O}$  before being placed in the next cleavable protein solution. This procedure was repeated until immobilised TEV protease activity had ceased.

Figure 6 (C) shows the sequential poly-histidine tag cleavage of *T. maritima* dihydrodipicolinate reductase (DHDPR), *A. thaliana* DHDPR, human peroxiredoxin 3 (PRX3), and *E. coli* DHDPS Y107W by TEV protease functionalised surface assembled amyloid fibril samples. On day one of the cleavage reactions, all of the bead samples showed some cleavage activity, with the SDS-PAGE gel showing very

similar results as Figure 6 (B). Again, the bead which was seeded, amyloid fibrils assembled, and TEV protease immobilised (lane 4) showed the highest TEV protease activity. The cleavage on day two had a very similar trend, but this time the amount of cleavage by the bead sample which was seeded, amyloid fibrils assembled, and TEV protease immobilised (lane 4), was much more pronounced compared to the other bead samples. By day three, the only bead sample retaining TEV protease activity was the bead sample which was seeded, amyloid fibrils assembled, and TEV protease immobilised (lane 4). This provides evidence that the presence of the surface assembled amyloid fibrils present protect TEV protease activity on the bead sample. By day four all of immobilised TEV bead samples showed no TEV protease activity. The control TEV protease reaction (lane 3) showed that the protein is cleavable, therefore the reason for no cleavage activity by the immobilised TEV protease beads samples could be due to inactivation of the immobilised TEV protease, or leaching of the immobilised TEV protease over time, which is known to be a problem when immobilising enzymes by physical adsorption.

### ***Conclusions***

Protein nanofibrils, such as amyloid fibrils can act as a versatile nanoscaffold by providing a large surface area for biomolecule immobilisation. In this work, immobilisation of TEV protease to insulin amyloid fibrils grown from the surface of a small glass bead, using physisorption, successfully immobilised active TEV protease. The catalytic activity of the immobilised TEV protease was preserved over three uses, with three different poly-histidine tagged proteins. Considering the immobilised TEV protease beads as a commercial proof-of-concept system, the results are promising taking into account that one 5 mm bead was used per reaction. Further optimisation of the surface amyloid fibril assembly and the enzyme immobilisation conditions could

increase the enzymatic activity, reusability and storage life of the immobilised TEV protease bead system, and optimisation of this technology towards smaller micro glass beads packed into a column could potentially increase the specific enzyme activity exponentially.

### ***Acknowledgements***

The authors would like to acknowledge Jackie Healy for expert technical expertise, once more with feeling. Funding for this work was received from the New Zealand Ministry of Business, Innovation, and Employment (Contract Number C02X0804)), the US Defense Threat Reduction Agency (Contract Number C02X0804), the MacDiarmid Institute for Advanced Materials and Nanotechnology, and Powerhouse Ventures.

## References

1. Cesaratto F, Burrone OR, Petris G. Tobacco Etch Virus protease: A shortcut across biotechnologies. *J Biotechnol*. 2016;231:239-249.
2. Waugh DS. Making the most of affinity tags. *Trends Biotechnol*. 2005;23(6):316-320.
3. Kapust RB, Tozser J, Copeland TD, Waugh DS. The P1' specificity of tobacco etch virus protease. *Biochem Biophys Res Commun*. 2002;294(5):949-955.
4. van den Berg S, Lofdahl P-A, Hard T, Berglund H. Improved solubility of TEV protease by directed evolution. *J Biotechnol*. 2006;121:291-298.
5. Blommel PG, Fox BG. A combined approach to improving large-scale production of tobacco etch virus protease. *Protein Expr Purif*. 2007;55(1):53-68.
6. Puhl AC, Giacomini C, Irazoqui G, Batista-Viera F, Villarino A, Terenzi H. Covalent immobilization of tobacco-etch-virus Nla protease: a useful tool for cleavage: of the histidine tag of recombinant proteins. *Biotechnol Appl Biochem*. 2009;53:165-174.
7. Waugh DS. TEV protease FAQ. Available at: [https://Mcll.Ncicrf.Gov/Waugh\\_tech/Faq/TeV.Pdf](https://Mcll.Ncicrf.Gov/Waugh_tech/Faq/TeV.Pdf); 2010.
8. Yu X, Sun J, Wang W, et al. Tobacco etch virus protease mediating cleavage of the cellulose-binding module tagged colored proteins immobilized on the regenerated amorphous cellulose. *Bioprocess Biosyst Eng*. 2017;40(7):1101-1110.
9. Miladi B, El Marjou A, Boeuf G, et al. Oriented immobilization of the tobacco etch virus protease for the cleavage of fusion proteins. *J Biotechnol*. 2012;158(3):97-103.
10. Wang H-C, Yu C-C, Liang C-F, Huang L-D, Hwu J-R, Lin C-C. Site-selective protein immobilization through 2-cyanobenzothiazole-cysteine condensation. *Chembiochem*. 2014;15(6):829-835.
11. Pilkington S, Roberts S, Meade S, Gerrard J. Amyloid fibrils as a nanoscaffold for enzyme immobilisation. *Biotechnol Prog*. 2010;26(1):93-100.
12. Raynes JK, Pearce FG, Meade SJ, Gerrard JA. Immobilization of organophosphate hydrolase on an amyloid fibril nanoscaffold: Towards bioremediation and chemical detoxification. *Biotechnol Prog*. 2011;27(2):360-367.
13. Sasso L, Sui S, Domigan L, et al. Versatile multi-functionalization of protein nanofibrils for biosensor applications. *Nanoscale*. 2014;6(3):1629-1634. doi:10.1039/c3nr05752f.

14. Kaur M, Roberts S, Healy J, et al. Crystallin Nanofibrils: A Functionalizable Nanoscaffold with Broad Applications Manufactured from Waste. *Chempluschem*. 2015;80(5):810-819.
15. Knowles TPJ, Mezzenga R. Amyloid fibrils as building blocks for natural and artificial functional materials. *Adv Mater*. 2016;28(31):6546-6561.
16. Hendler N, Belgorodsky B, Mentovich ED, Richter S, Fadeev L, Gozin M. Multiple self-assembly functional structures based on versatile binding sites of beta-lactoglobulin. *Adv Funct Mater*. 2012;22(18):3765-3776.
17. Lazar I. *GelAnalyzer*.; 2010. GelAnalyzer.com.
18. Abràmoff MD, Magalhães PJ, Ram SJ. Image processing with ImageJ. *Biophotonics Int*. 2004;11(7):36–42.
19. Nielsen L, Khurana R, Coats A, et al. Effect of environmental factors on the kinetics of insulin fibril formation: Elucidation of the molecular mechanism. *Biochemistry*. 2001;40(20):6036-6046.
20. LeVine III H. Thioflavin T interaction with synthetic Alzheimer's disease  $\beta$ -amyloid peptides: Detection of amyloid aggregation in solution. *Protein Sci*. 1993;2(3):404-410.21. Schmit JD, Ghosh K, Dill K. What drives amyloid molecules to assemble into oligomers and fibrils? *Biophys J*. 2011;100(2):450-458.
22. Nilsson MR. Techniques to study amyloid fibril formation in vitro. *Methods*. 2004;34(1):151-160.
23. Ha C, Park CB. Template-directed self-assembly and growth of insulin amyloid fibrils. *Biotechnol Bioeng*. 2005;90(7):848-855.
24. Howarter JA, Youngblood JP. Optimization of silica silanization by 3-aminopropyltriethoxysilane. *Langmuir*. 2006;22(26):11142-11147. doi:10.1021/la061240g.
25. Morpurgo M, Bayer EA, Wilchek M. N-hydroxysuccinimide carbonates and carbamates are useful reactive reagents for coupling ligands to lysines on proteins. *J Biochem Biophys Methods*. 1999;38(1):17-28.
26. Jarrett J, Lansbury P. Amyloid fibril formation requires a chemically discriminating nucleation event - studies of an amyloidogenic sequence from the bacterial protein OsmB. *Biochemistry*. 1992;31(49):12345-12352.
27. Xue W, Hellewell A, Gosal W, Homans S, Hewitt E, Radford S. Fibril fragmentation enhances amyloid cytotoxicity. *J Biol Chem*. 2009;284(49):34272-34282.
28. Domigan LJ, Healy J, Meade SJ, Blaikie RJ, Gerrard JA. Controlling the dimensions of amyloid fibrils: Towards homogenous components for bionanotechnology. *Biopolymers*. 2011;97(2):123-133.



29. Zlateski V, Fuhrer R, Koehler FM, et al. Efficient magnetic recycling of covalently attached enzymes on carbon-coated metallic nanomagnets. *Bioconjug Chem.* 2014;25(4):677-684.
30. Alaa A. A. Aljabali, Alaa A A Barclay, J Elaine Steinmetz, Nicole F Lomonossoff, George P Evans. Controlled immobilisation of active enzymes on the cowpea mosaic virus capsid. *Nanoscale.* 4(18):5640–5645.